

Characteristics of a Type of NTC Thermistors for Cryogenic Applications

Yuqi Lan^{1,2*}, Shenyin Yang², Guangming Chen¹, Sifeng Yang²

¹Institute of Refrigeration and Cryogenics, Zhejiang University, Hangzhou, China

²Beijing Institute of Aerospace Testing Technology, Beijing, China

Email: *hangtiandiwen@163.com

How to cite this paper: Lan, Y.Q., Yang, S.Y., Chen, G.M. and Yang, S.F. (2020) Characteristics of a Type of NTC Thermistors for Cryogenic Applications. *Advances in Materials Physics and Chemistry*, 10, 167-177.
<https://doi.org/10.4236/ampc.2020.108012>

Received: July 15, 2020

Accepted: August 14, 2020

Published: August 17, 2020

Copyright © 2020 by author(s) and Scientific Research Publishing Inc. This work is licensed under the Creative Commons Attribution International License (CC BY 4.0).

<http://creativecommons.org/licenses/by/4.0/>



Open Access

Abstract

A new type of miniature negative temperature coefficient (NTC) thermistors has been developed and manufactured with Mn-Ni-Cu-Fe oxides. The prepared NTC thermistors were calibrated in the temperature range from 77 K to 300 K with 1 μ A exciting currents. The automatic calibration apparatus as well as thermometric characteristics, stability, calibration equations and interchangeability of the manufactured thermistors were investigated. A mean fit equation was obtained: $1/T = 8.60 \times 10^{-4} + 6.54 \times 10^{-4} \ln(R/R_{ref}) + 2.46 \times 10^{-5} \ln(R/R_{ref})^2 + 9.48 \times 10^{-7} \ln(R/R_{ref})^3 - 2.16 \times 10^{-8} \ln(R/R_{ref})^4$. All the prepared NTC thermistors agreed with this fit with an error of 1.5 K. If the greater accuracy is required, a calibration is necessary, and the calibration accuracy is estimated to be ± 10 mK.

Keywords

Thermometer, Cryogenics, Thermistors, Calibration, Cryostat

1. Introduction

Many cryogenic applications require a large number of temperatures to be monitored in various areas of cryogenic engineering and low-temperature physics. The two most commonly used parameters in cryogenic thermometers are voltage and resistance. The widely applied cryogenic temperature sensors include thermocouples, diodes, resistors and capacitors and so on. Resistors can be classified as positive temperature coefficient (PTC) or negative temperature coefficient (NTC) [1] [2] [3]. NTC resistors exhibit a decrease in resistance with an increase in temperature, which is highly resistant to magnetic field-induced errors and ionizing radiation. Most adapted and commercially available for applications in high magnetic fields and radiation are made of carbon, carbon-glass

and carbon ceramic, fabricated from bulk materials, and films based on ruthenium oxide, and zirconium oxy-nitride. However, their price is high. Therefore, we investigated the feasibility of low-cost NTC thermistors [4] [5] [6].

The advantages of NTC thermistors for temperature measurement are the high sensitivity to yield a high resolution and the high resistivity permits small mass units with fast response. This makes them compatible for using requiring a high output signal over a relatively narrow temperature range [7] [8]. Low-temperature (173 K to 400 K) NTC thermistors made of transition metal oxides are applied in industries for temperature measurement, control and compensation in electronic devices. However, cryogenic NTC thermistors for applications below 173 K have been scarcely reported in detail.

In this paper, the Mn-Ni-Cu-Fe oxides NTC thermistors of low resistivity were prepared by using the solid-state coordination reaction route, with the *in-situ* lead wire attachment method (ISAM) and sealed by glass, as described in our previous work [7]. The thermistors were calibrated with a stable exciting current. The thermistors provide good sensitivity over the measurement range from 77 K to 300 K. And meanwhile, the automatic calibration apparatus, stability, calibration equations and interchangeability of prepared thermistors were also investigated.

2. Manufacturing Technology of Thermistors

The NTC ceramics were synthesized through solid-state route. Analytical grade nickel acetate $\text{Ni}(\text{CH}_3\text{COO})_2 \cdot 4\text{H}_2\text{O}$, copper acetate $\text{Cu}(\text{CH}_3\text{COO})_2 \cdot \text{H}_2\text{O}$, manganese acetate $\text{Mn}(\text{CH}_3\text{COO})_2 \cdot 4\text{H}_2\text{O}$, iron oxalate $\text{FeC}_2\text{O}_4 \cdot 2\text{H}_2\text{O}$ and oxalic acid $\text{H}_2\text{CO}_4 \cdot 2\text{H}_2\text{O}$ were used as raw materials. The contents of metal ions in raw materials are determined by chemical analysis. The raw materials were accurately weighed according to their molar ratio, transferred to polypropylene jars and milled for 24 h using zirconia balls as milling medium to get a uniform mixture. The milled was dried at 75 °C, and calcined at 800 °C for 4 h in air. The calcined powder was then ground for 48 h by ball milling to get a narrow particle-size distribution.

Disk-shaped thermistors were designed by using *in-situ* lead wire attachment method (ISAM). Celluloid board with a height of 2.0 mm was drilled a row of holes with a diameter of about 3.5 mm, and a distance of about 2.5 mm between holes, then was grooved at both sides of the centres of holes, and the distance of between two grooves with the depth of 1.0 mm and the width of 0.05 mm is 2 mm. Two platinum lead wires (0.05 mm diameter) were placed into two grooves. The powders granulated with a 4% polyvinyl alcohol (PVA) organic binder were placed in the holes to form green bodies with cold-pressed using a steel die by single-end compaction and pressed at 200 MPa by isopressing process. Celluloid board with green bodies were heated in air to 400 °C at a rate of 100 °C/h, kept at that temperature for 2 h for adequate binder burnout, and subsequently heated to 1150 °C at a rate 200 °C/h and kept at that temperature for 4 h for sintering.

The sintered samples were cut, and subsequently soldered copper leads and sealed by glass. So, NTC thermistors were manufactured. **Figure 1** shows the schematic of the *in-situ* lead wire attachment method (ISAM) for manufacturing thermistors [9].

XRD pattern of the sintered experimental sample in **Figure 2** shows the presence of single-phase cubic spinel nickel manganite. The SEM microstructure obtained from the surface of the sample sintered at 1150°C is given in **Figure 3**. It is seen that uniformly sized grains are formed during sintering. The amount of porosity is very less, which shows a dense microstructure formation.

3. Automatic Calibration Apparatus

Scarcely any description of the calibration device has presented in the literature, and a simple statement of the calibration device is given here. The automatic calibration apparatus, which was manufactured by Institute of Refrigeration and Cryogenics, Zhejiang University, in 2008, is now in the ownership of Beijing Institute of Aerospace Testing Technology. The automatic calibration equipment consists of three main parts, including cryostat, temperature control system and

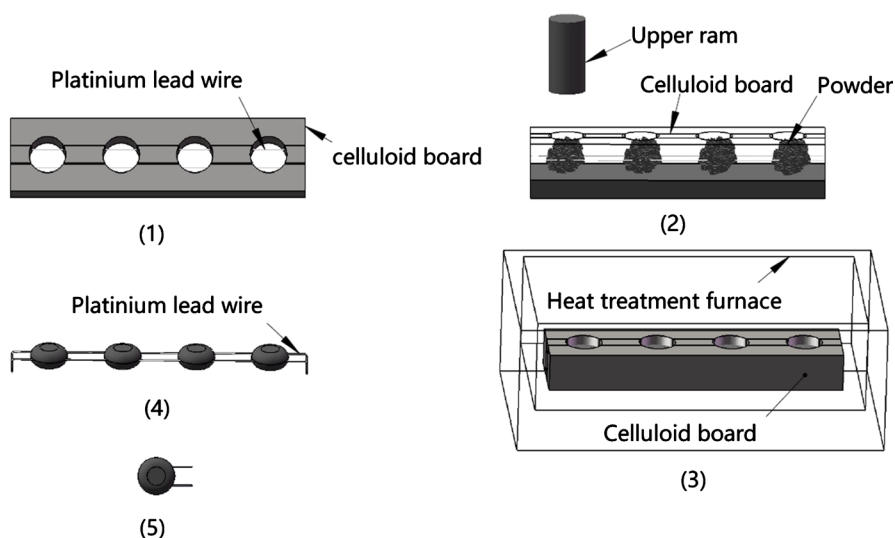


Figure 1. Schematic of *in-situ* lead wire attachment method for fabrication of thermistors.

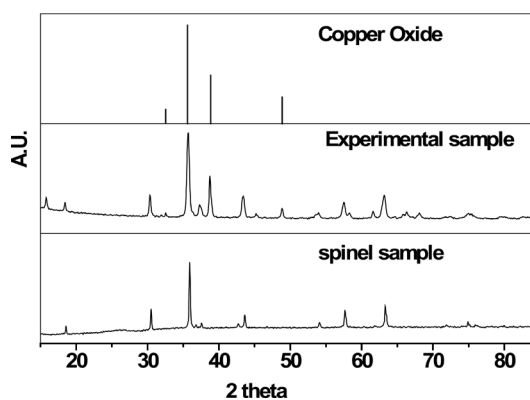


Figure 2. XRD patterns of sintered samples, Copper Oxide and spinel sample.

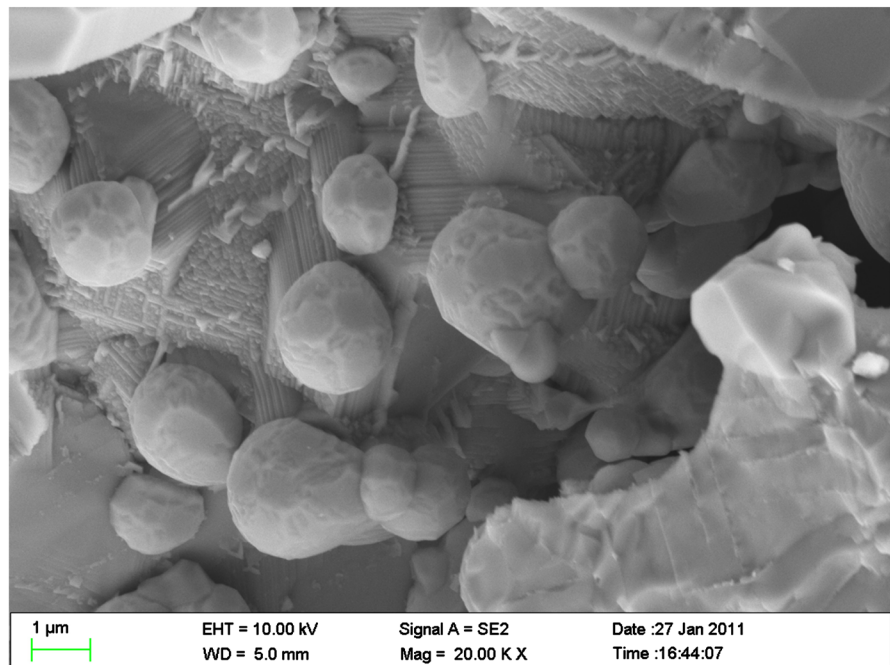


Figure 3. Scanning electron micrographs of surface of the sintered samples.

data acquisition system. Schematic illustration of the automatic calibration facility is shown in **Figure 4**. The cryostat consists of dewar, evacuation system, vacuum chamber, constant-temperature block, heat sink and some important accessories. The constant-temperature block are uniformly drilled holes on the bottom surface, and hung in an Indium-sealed vacuum can with adiabatic strings in order to reduce the heat leak. A Standard Capsule Platinum Resistance Thermometer (SCPRT, Tinsley 5187L, calibrated by National Institute Metrology of china with the expand uncertainty of 2 mK) and thermometers were immersed into the holes of the block by silicon grease to guarantee good thermal contact with the block. The leads to each sensor are 6 m long, and are wound around the heat sink mounted on the top of vacuum can, before reaching a final heat sink on the constant-temperature block. The temperature control system includes a Lakeshore-331s Temperature controller, a Fluke. Model 1590 Supper thermometer II and computer. The computer collects the signals of SCPRT monitored by the Fluke. Model 1590 Supper thermometer II. The control program programmed with Visual Basic regulates the power output of the Lakeshore-331s Temperature controller to heat the heating wire wrapped tightly around the surface the upper part of the constant-temperature block. The segmented Fuzzy-PID (proportional-integral-differential) algorithm is applied in the program. The temperature fluctuation of the cryostat is smaller than 3 mK with 30 min. Data acquisition system consists of Keithley-2400 Source-meter, Keithley-2700 Multi-function meter and the computer. A stable current supplied by Keithley-2400 was applied to the calibrated resistance thermometers. The voltage signals of those thermometers to be calibrated are collected by the computer and stored for the further analysis [10] [11] [12] [13].

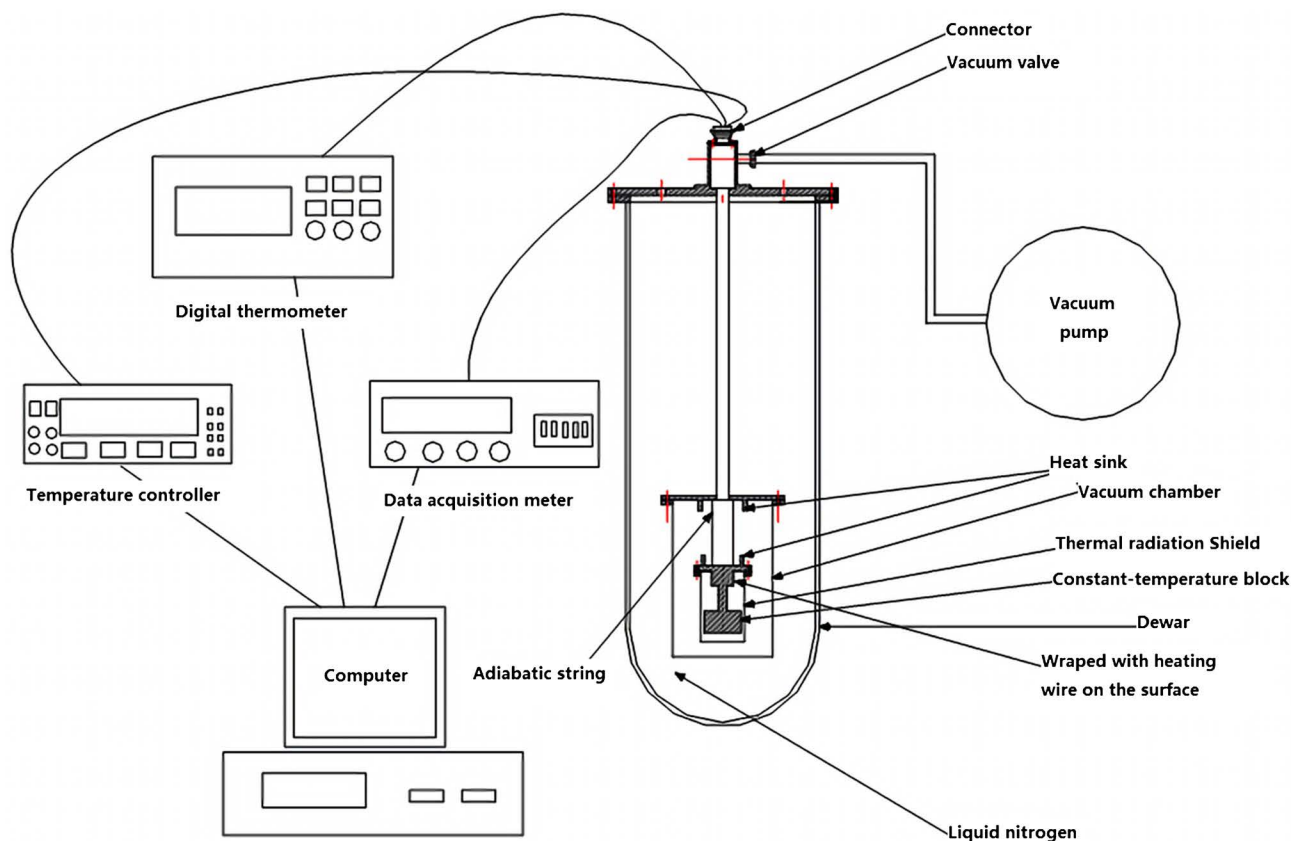


Figure 4. Schematic diagram of the automatic calibration system.

4. Characteristics of NTC Thermistors

4.1. Thermometric Characteristics

Six thermistors were mounted in the constant-temperature block of the cryostat and driven with a $1 \mu\text{A}$ current. The SCPRT reference thermometer placed in the constant-temperature block was measured by the Fluke, Model 1590 Super thermometer II. The thermistors calibration was carried out by recording those voltages of calibrated thermistors and reference temperature in the temperature from 77 K to 120 K with 5 K intervals and with 20 K intervals from 120 K to 300 K. The calibration tables were obtained by interpolating the calibration data, and averaged to obtain a mean curve. **Figure 5** shows the dependence of resistance on the temperature of the six thermistors with the $1 \mu\text{A}$ driving current. The thermistors resistance depends smoothly on over the temperature range. The variation in thermometric characteristics among thermistors results from the difference of manufacturing techniques.

What shown in **Figure 6** is sensitivity, $|S| = |dR/dT|$, as functions of temperature in the 77 K~300 K temperature range. The thermistors are more sensitive at temperatures from 77 K to 140 K. The values of resistance, sensitivity between manufactured NTC thermistors and other thermistors from Lake Shore Company at typical temperature are presented in **Table 1**. The prepared NTC thermistors have extremely high resistance and sensitivity in the calibrated tem-

perature range, which is concluded by comparing those data.

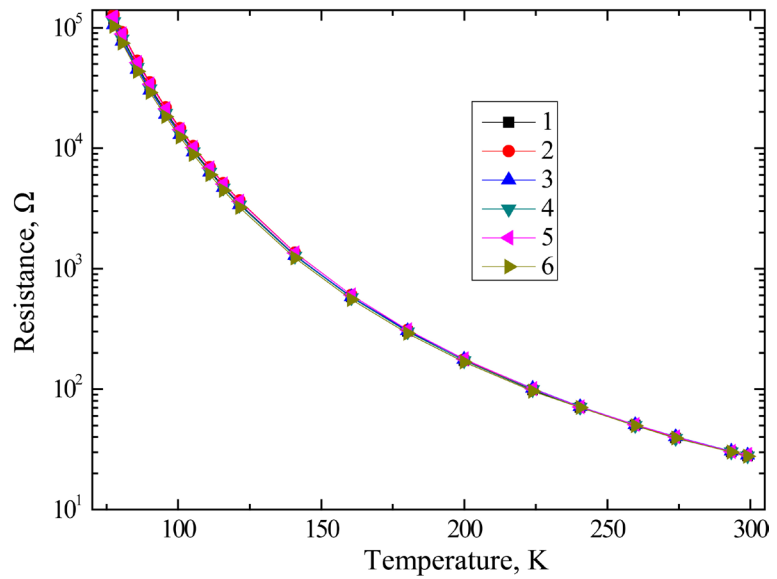


Figure 5. The typical temperature dependences of the six calibrated thermistors.

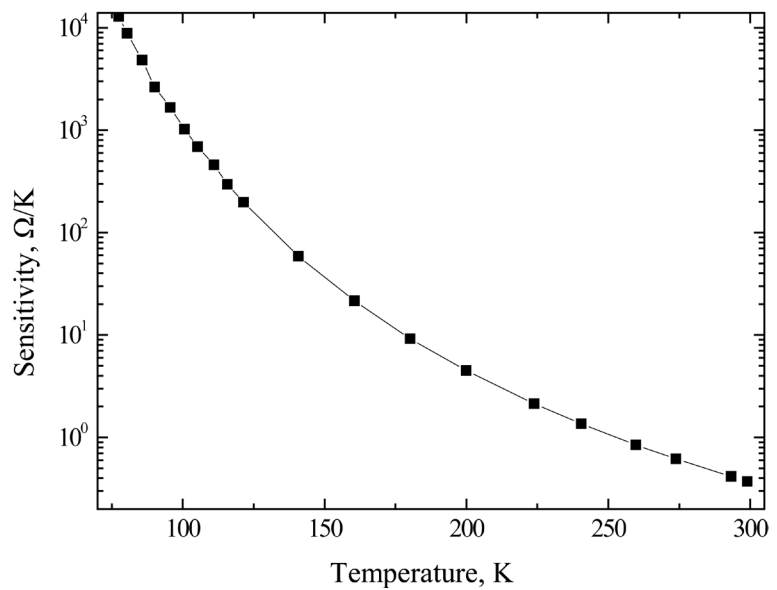


Figure 6. Sensitivity, $|S|=|dR/dT|$, versus temperature curves for the ten prepared thermistors.

Table 1. The values of resistance, sensitivity between NTC thermistors and different NTC RTDs from Lake Shore Company at typical temperatures

T(K)	NTC thermistors		CX-1080		GR-200A-1500		CGR-1-2000	
	R(Ω)	dR/dT (Ω/K)	R (Ω)	dR/dT (Ω/K)	R (Ω)	dR/dT (Ω/K)	R (Ω)	dR/dT (Ω/K)
77	109,000	-12338.4	836	-115.39	5.01	-0.078	21.65	-0.157
100	14200	-1095.76	-	-	3.85	-0.033	-	-
300	27.6	-0.365	130	-0.55	-	-	11.99	-0.015

4.2. Stability

Stability is the closeness of agreement between the results of the measurements of the same measurand carried out under changed conditions of measurements. Preliminary investigation of stability of NTC thermistors at 77 K was performed. Together with the six calibrated thermistors were immersed in liquid nitrogen for 300 h, and short-term stability data was obtained by subjecting NTC thermistors to 50 thermal shocks from 473 K to 77 K. Finally, resistance shifts were measured at 77 K in liquid nitrogen. Deviations of the thermistors resistance corresponded to temperature error in the range from 0.9 mK to 4.7 mK. Long-term stability data was obtained by subjecting NTC thermistors to 200 thermal shocks from ambient to liquid nitrogen. The long-term stability for themistors corresponded to temperature error not more than ± 8 mK at 77 K. Compared with Germanium, CernoxTM, and Carbon-Glass RTDs, therefore, the stability of NTC thermistors may be much better.

4.3. Calibration Equations of Thermistors

As well to known, the performance of the thermistors for temperature measurement is affected by the calibration equation. Chiachung Chen [8] considered the Hoge-3 equation,

$1/T = A_0 + A_1 \ln(R/R_{\text{ref}}) + A_2 \ln(R/R_{\text{ref}})^2 + A_3 \ln(R/R_{\text{ref}})^3 + A_4 \ln(R/R_{\text{ref}})^4$, was the best equation for thermistors by evaluating seven calibration equations. Here, R is the specific resistance ohm value, R_{ref} is 1 ohm, and T is the absolute temperature. The software, MATLAB R2006a, is used to estimate the parameters of calibration equations. The e_i was defined as follow: $e_i = T_i - \hat{T}_i$, where e_i is the error of calibration equation, T_i is the dependent temperature variable and \hat{T}_i is the predicted values of calibration equation. Four statistics, e_{max} , e_{min} , $|e|_{\text{ave}}$ and e_{std} are adopted to evaluated the precision of equation. The e_{max} is the maximum e_i value and the e_{min} is the minimum e_i value. The $|e|_{\text{ave}}$ was defined as follow: $|e|_{\text{ave}} = \frac{\sum |e_i|}{n}$, where $|e_i|$ is the absolute value of e_i , n is the number of data. The uncertainty from a calibration equation can be calculated

from the standard deviation of the calibration equation: $e_{\text{std}} = \left(\frac{(e_i - \bar{e}_i)^2}{n-1} \right)^{0.5}$,

where \bar{e}_i is the average of e_i . The values of estimated parameters, e_{max} , e_{min} , $|e|_{\text{ave}}$ and e_{std} of calibration equation for six NTC thermistors are listed in **Table 2**. The e_{max} , e_{min} , $|e|_{\text{ave}}$ and e_{std} values are relatively small, which show the Hoge-3 equation has good precision performance for prepared thermistors. The residual plots the calibration equation for the six thermistors are presented in **Figure 7**.

4.4. Interchangeability

It is very convenient and cost effective to have temperature sensors that match a standard curve, thus not requiring individual calibration. The mean calibration

table of the thermistors for the temperature range from 77 K to 300 K is of most interest to us for the future use. So mean table of resistance versus temperature of the six calibrated thermistors was established, and fitted with the Hoge-3 equation. A mean fit equation was obtained: $1/T = 8.60 \times 10^{-4} + 6.54 \times 10^{-4} \ln(R/R_{\text{ref}}) + 2.46 \times 10^{-5} \ln(R/R_{\text{ref}})^2 + 9.48 \times 10^{-7} \ln(R/R_{\text{ref}})^3 - 2.16 \times 10^{-8} \ln(R/R_{\text{ref}})^4$. **Figure 6** shows

Table 2. The values of estimated parameters, e_{max} , e_{min} , $|e|_{\text{ave}}$ and e_{std} of calibration equation for six NTC thermistors.

Sample No.	Parameters	e_{max} (mK)	e_{min} (mK)	$ e _{\text{ave}}$ (mK)	e_{std} (mK)	
1	A0	8.64×10^{-4}	9.6	-5.1	2.53	3.41
	A1	6.59×10^{-4}				
	A2	2.35×10^{-5}				
	A3	1.06×10^{-6}				
	A4	-2.26×10^{-8}				
2	A0	9.18×10^{-4}	8.31	-7.36	3.03	3.98
	A1	6.45×10^{-4}				
	A2	2.37×10^{-5}				
	A3	9.28×10^{-7}				
	A4	-1.99×10^{-8}				
3	A0	8.11×10^{-4}	7.87	-6.25	2.84	3.60
	A1	6.62×10^{-4}				
	A2	2.30×10^{-5}				
	A3	1.21×10^{-6}				
	A4	-2.84×10^{-8}				
4	A0	8.26×10^{-4}	9.12	-6.74	2.45	3.45
	A1	6.57×10^{-4}				
	A2	2.63×10^{-5}				
	A3	7.90×10^{-7}				
	A4	-1.87×10^{-8}				
5	A0	8.85×10^{-4}	7.77	-4.94	2.49	3.21
	A1	6.43×10^{-4}				
	A2	2.55×10^{-5}				
	A3	8.20×10^{-7}				
	A4	-1.77×10^{-8}				
6	A0	8.56×10^{-4}	9.96	-5.98	2.90	3.78
	A1	6.56×10^{-4}				
	A2	2.55×10^{-5}				
	A3	9.74×10^{-7}				
	A4	-2.28×10^{-8}				

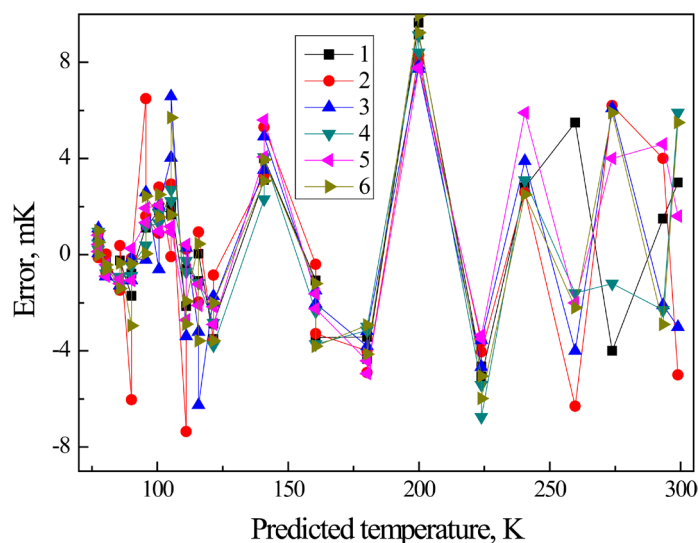


Figure 7. The residual plots of calibration equation for six NTC thermistors.

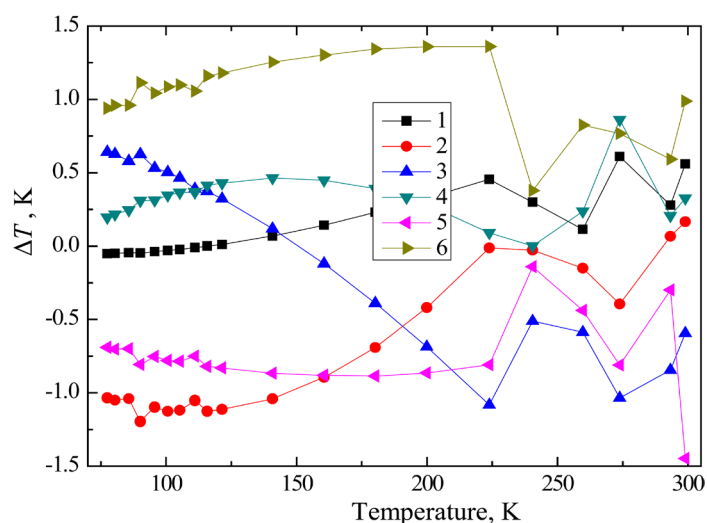


Figure 8. The dependence of the temperature deviation ΔT of the six calibrated NTC thermistors from their mean fit curve on the temperature.

the dependence of the temperature deviation ΔT of the six calibrated NTC thermistors from their mean fit curve on the temperature. The deviations from the mean curve are combined with the variation among the NTC thermistors, which is concluded that application of the mean curve will result in a measurement of error of ± 1.5 K in the temperature range from 77 K to 300 K. Therefore, to significantly improve on accuracy, specific calibration of the prepared NTC thermistors is required, and the calibration accuracy is estimated to be ± 10 mK, which is shown in **Figure 8**.

5. Conclusion

A new type of NTC thermistors had been designed, manufactured and calibrated in the temperature range from 77 K to 300 K. They showed good thermometric properties, stability and high thermal sensitivity. The accuracy and precision of

the prepared thermistors with the Hoge-3 equation fit were as good as other commercial NTC Resistors. A mean fit equation was obtained: $1/T = 8.60 \times 10^{-4} + 6.54 \times 10^{-4} \ln(R/R_{\text{ref}}) + 2.46 \times 10^{-5} \ln(R/R_{\text{ref}})^2 + 9.48 \times 10^{-7} \ln(R/R_{\text{ref}})^3 - 2.16 \times 10^{-8} \ln(R/R_{\text{ref}})^4$. All the prepared NTC thermistors agreed with this fit with an error of 1.5 K. If the greater accuracy is required, a calibration is necessary, and the calibration accuracy is estimated to be ± 10 mK. Therefore, their widespread application is important in cryogenic engineering and experimental physics.

Acknowledgements

This work was supported in part by Beijing Institute of Aerospace Testing Technology and Material Physics and Chemistry Research Center of the Xingjiang Technical Institute of Physics and Chemistry, the Chinese Academy of Science. The authors are grateful to Ying Wang, Xue Dong and Dongfang Wang for measuring the six prepared thermistors.

Conflicts of Interest

The authors declare no conflicts of interest regarding the publication of this paper.

References

- [1] Brandt, B.L., Liu, D.W. and Rubin, L.G. (1999) Low Temperature Thermometry in High Magnetic Fields. VII. Cernox™ Sensors to 32 T. *Review of Scientific Instruments*, **70**, 104. <https://doi.org/10.1063/1.1149549>
- [2] Wang, C.C., Akbar, S.A., Chen, W. and Schorr, J.R. (1997) High-Temperature Thermistors Based on Yttria and Calcium Zirconate. *Sensors and Actuators A*, **58**, 237. [https://doi.org/10.1016/S0924-4247\(97\)01394-0](https://doi.org/10.1016/S0924-4247(97)01394-0)
- [3] Boltovets, N.S., Kholevchuk, V.V., Konakova, R.V., Mitin, V.F. and Venger, E.F. (2001) Ge-Film Resistance and Si-Based Diode Temperature Microsensors for Cryogenic Applications. *Sensors and Actuators A*, **92**, 191-196. [https://doi.org/10.1016/S0924-4247\(01\)00562-3](https://doi.org/10.1016/S0924-4247(01)00562-3)
- [4] Ruby, R.L. and Kempson, M. (1996) Cryogenic Temperature Measurement. *Revue Générale de Thermique*, **35**, 338-343. [https://doi.org/10.1016/S0035-3159\(99\)80076-2](https://doi.org/10.1016/S0035-3159(99)80076-2)
- [5] Minti, V.F., Kholevchuk, V.V. and Kolodych, B.P. (2011) Ge-on-GaAs Film Resistance Thermometers: Low-Temperature Conduction and Magnetoresistance. *Cryogenics*, **51**, 68-73. <https://doi.org/10.1016/j.cryogenics.2010.11.003>
- [6] Minti, V.F., Venger, E.F., Boltovets, N.S., Oszwaldowski, M. and Berus, T. (1998) Low-Temperature Ge Film Resistance Thermometers. *Sensors and Actuators A*, **68**, 303-306. [https://doi.org/10.1016/S0924-4247\(98\)00023-5](https://doi.org/10.1016/S0924-4247(98)00023-5)
- [7] Shieh, J., Huber, J.E., Fleck, N.A. and Ashby, M.F. (2011) The Selection of Sensors. *Progress in Materials Science*, **46**, 461-504. [https://doi.org/10.1016/S0079-6425\(00\)00011-6](https://doi.org/10.1016/S0079-6425(00)00011-6)
- [8] Chen C.C. (2009) Evaluation of Resistance-Temperature Calibration Equations for NTC Thermistors. *Measurement*, **42**, 1103-1111. <https://doi.org/10.1016/j.measurement.2009.04.004>
- [9] Lan, Y.Q., Yu, L.H., Chen, G.M., Yang, S.F. and Chang, A.M. (2010) Construction

-
- and Characterization of NTC Thermistors at Low Temperature. *International Journal of Thermophysics*, **31**, 1456-1465.
<https://doi.org/10.1007/s10765-010-0790-0>
- [10] Ricketson, B.W.A. and Watkins, R.E.J. (2009) The 27 Ω Rhodium-Iron Ceramic Sensor. *Cryogenics*, **49**, 320-325. <https://doi.org/10.1016/j.cryogenics.2009.03.006>
- [11] Chen, G.M., Gao, X., Zhang, S.Z., Chen, Q. and Lan, Y.Q. (2010) Development of an Automatic Calibration Device for High-Accuracy Low Temperature Thermometers. *Science China Technological Sciences*, **53**, 2404-2407.
<https://doi.org/10.1007/s11431-010-4020-6>
- [12] Zhang, P., Xu, Y.X., Wang, R.Z. and Murakami, M. (2003) Fractal Study of the Fluctuation Characteristic in the Calibration of the Cryogenic Thermocouples. *Cryogenics*, **43**, 53-58. [https://doi.org/10.1016/S0011-2275\(03\)00004-3](https://doi.org/10.1016/S0011-2275(03)00004-3)
- [13] Rijpma, A.P. and ter Brake, H.J.M. (2006) Cryogenic Thermometry with a Common Diode: Type BAS16. *Cryogenics*, **46**, 68-69.
<https://doi.org/10.1016/j.cryogenics.2005.11.009>